Available online at www.sciencedirect.com
ScienceDirect
Ceramics International 34 (2008) 1431–1438
CERAMICS INTERNATIONAL
www.elsevier.com/locate/ceramint

Development of blue ceramic dyes from cobalt phosphates

S. Meseguer, M.A. Tena *, C. Gargori, R. Galindo, J.A. Badenes, M. Llusar, G. Monrós

Inorganic Chemistry Area, Inorganic and Organic Chemistry Department, Jaume I University, Castellón, Spain

Received 20 October 2006; received in revised form 5 March 2007; accepted 2 April 2007
Available online 7 May 2007

Abstract

In this study the development of blue ceramic dyes from compositions based on phosphate structures have been investigated. The replacement of cobalt by copper or iron to minimize the Co content have been considered. $MFeO(PO_4)$ (M = Co, Cu) solid solutions have been obtained with $Co_{1-x}Cu_xFeOPO_4$ ($0 \leq x \leq 1$) compositions prepared from gels and fired at 1000 °C/2 h. $Co_{1-x}Cu_xFeOPO_4$ compositions are not indicated to minimize the Co content in ceramic dyes because they decompose in glazed samples and pinhole defect is obtained. From $FeCoOPO_4$–$2FePO_4$ compositions, $Co_3Fe_4(PO_4)_6$ structure introduces the Co^{2+} ions into glassy matrix and suitable blue materials are obtained. In the conditions of this study, optimal cobalt amount is about 10 wt% Co from $Co_{1-x}Fe_{1+x}O_{1-x}(PO_4)_{1+x}$ ($x \approx 0.6$) compositions.
© 2007 Elsevier Ltd and Techna Group S.r.l. All rights reserved.

Keywords: A. Sol–gel processes; C. Color; D. Traditional ceramics

1. Introduction

Cobalt usually occurs in association with other metals such as copper, nickel, manganese and arsenic. Small amounts are found in most rocks, soil, surface and underground water, plants and animals. Cobalt and its compounds are used to prepare alloys [1], in the drying of alkyd paints [2], catalysts [3], porcelain enamelling [4], cements [5] and ceramic pigments [6]. The radioactive isotope Cobalt 60 is used in treating patients in nuclear medicine and in research [7]. Natural cobalt can stay in the air for a few days, but it will stay for years in water and soil. Cobalt is not often freely available in the environment, but when cobalt particles are not bound to soil or sediment particles the uptake by plants and animals is higher and accumulation in plants and animals may occur [8]. Cobalt is beneficial for humans because it is a part of vitamin B_{12}, which is essential for human health. However, too high concentrations of cobalt may damage human health. The International Agency for Research on Cancer has determined that cobalt is a possible carcinogen to humans (2B: possibly carcinogenic to humans) [9].

Cobalt is scarce in the earth. Its ores are geographically localized, and it has a difficult metallurgy. This makes the element expensive.

The traditional source of blue in ceramic pigments is the cobalt ion [10], except for vanadium-zircon turquoise blue (14-42-2 DCMA). The Co_2SiO_4 olivine (5-08-2 DCMA), $(Co,Zn)_2SiO_4$ willemite (7-10-2 DCMA), $CoAl_2O_4$ spinel (13-26-2 DCMA), Co_2SnO_4 (13-27-2 DCMA), $(Co,Zn)Al_2O_4$ (13-28-2 DCMA) and $Co(Al,Cr)_2O_4$ (13-28-2 DCMA) are further blue pigments. Some of them are widely used in the ceramic industry. There are two ceramic pigments with phosphate structure in the DCMA classification [11]. They are cobalt violet phosphate (8-11-1 DCMA) and cobalt lithium violet phosphate (8-12-1 DCMA). Synthesis from industrial-waste and attempt to minimize the cobalt amount have been reported [12–15]. Solid solutions are important in the design of new materials that have specific properties. Preparation of compositions with low Co content seems to be possible from solid solution formation. Thus, a nice palette of blue ceramic pigments with different color intensities can be obtained based on the willemite lattice with 25 −2.5 Co mol% [14]. In blue ceramic dyes from phosphates, $Co_3(PO_4)_2$ and $Co_2P_2O_7$ structures introduce the Co^{2+} ions into glassy matrix. These structures are dissolved but ions remain in glazed samples. The blue color of glazed samples is attributed to Co^{2+} ions. $Co_{3-x}Fe_xP_2O_{8+x/2}$ compositions with $0 \leq x \leq 1.0$ (between 48 and 32 wt% Co) and $Co_xFe_{1-x}PO_{4-x/2}$

* Corresponding author. Tel.: +34 964728249; fax: +34 964728214.
E-mail address: tena@qio.uji.es (M.A. Tena).

0272-8842/$34.00 © 2007 Elsevier Ltd and Techna Group S.r.l. All rights reserved.
doi:10.1016/j.ceramint.2007.04.008

compositions with $0.30 \leq x \leq 0.50$ (about 12–20 wt% Co) can be considered to minimize the Co content in blue ceramic dyes [15]. $CoFeOPO_4$ was detected from $Co_{3-x}Fe_xP_2O_{8+x/2}$ compositions when iron amount is high. This structure seems to be suitable to introduce the Co^{2+} ions into glassy matrix and to minimize cobalt amount.

The ceramic pigments industry tends towards cheap and simple processing. The synthesis from mixtures of solid starting materials is habitual. The use of CoO and cobalt salts as raw materials in synthesis of ceramic pigments requires high temperature to decompose the Co_3O_4 compound formed from them. Pinhole defect is obtained from glazed samples when Co_3O_4 is present in ceramic pigment. Co_2SiO_4 olivine is widely used in the ceramic industry. Temperature to obtain olivine (and willemite or spinel) is about 1300 °C. Co_2SiO_4 olivine did not remain stable in glaze during firing [13]. In the cobalt precursors of blue ceramic materials, the synthesis temperature can be reduced by the use of cobalt phosphates. $Co_3(PO_4)_2$, $Co_2P_2O_7$ or $FePO_4$ compounds can be obtained (without to make expensive the synthesis) at $T \leq 1000$ °C [15].

In the orthorhombic crystal structure of $CoFeOPO_4$, the phosphorus atoms are at the centre of PO_4 tetrahedra that are not connected between them. The Co^{2+} and Fe^{3+} ions are in the centre of distorted octahedra. These ions are located in two different crystallographic sites, 4a and 4c, respectively, of the orthorhombic cell. This structure can be described as zigzag chains along b of alternating $Co^{2+}O_6$ and $Fe^{3+}O_6$ octahedra sharing a face. The phosphorus atoms occupy interstitial tetrahedra between adjacent chains. The adjacent chains share also the oxygen O(1) that is an important element for the exchange interactions in compounds with this structure [16]. The oxyphosphates $MFeOPO_4$ (M: Co^{2+}, Ni^{2+}, Cu^{2+}) are isomorphic to the mixed valence compound α-Fe_2OPO_4 with space-group *Pnma*.

The aim of this study is to investigate the development of blue color in ceramic materials from compositions based on $CoFeOPO_4$ structure and to establish the compositional range of these prepared samples for which the materials develop blue colorations in glazes or stoneware matrix. Replacement of cobalt by copper or iron is considered to minimize the Co content of the dye. Results from this study are compared with results obtained in a previous study from compositions based on $FePO_4$ structure.

2. Experimental procedures

$Co_{1-x}Cu_xFeOPO_4$ ($0 \leq x \leq 1$) and $Co_{1-x}Fe_{1+x}O_{1-x}(PO_4)_{1+x}$ ($0 \leq x \leq 1$) compositions were prepared by the sol–gel method to investigate the possibility of formation of solid solutions, the replacement of cobalt in $CoFeOPO_4$ structure by copper or iron, respectively and the coloration of the development of blue coloration in glazed samples. The starting materials were $Co(NO_3)_2{\cdot}6H_2O$ (Merck), $Fe(NO_3)_3{\cdot}9H_2O$ (Merck), $Cu(NO_3)_2{\cdot}2.5H_2O$ (Merck) and H_3PO_4 (Panreac) of reagent grade chemical quality. A 0.67 M aqueous solution of $Co(NO_3)_2$ and $Fe(NO_3)_3$ or $Cu(NO_3)_2$ was added on a 0.67 M solution of H_3PO_4 in water. After that, a solution of ammonium hydroxide was added dropwise until that gelation occurred (pH 7–8). Finally, the gel was dried by an infrared lamp and the dried samples were fired in refractory crucibles. $Co_{1-x}Cu_xFeOPO_4$ samples were also prepared by the ceramic method from Co_2O_3 (Merck), CuO (Merck), Fe_2O_3 (Merck) and H_3PO_4 (Panreac) of reagent grade chemical quality. $Co_{1-x}Cu_xFeOPO_4$ compositions were fired at 800, 900 and 1000 °C for 48 h of soaking times at each temperature and $Co_{1-x}Fe_{1+x}O_{1-x}(PO_4)_{1+x}$ compositions were fired at 800 and 1000 °C for 2 h of soaking times at each temperature.

The resulting materials were examined with a Siemens D5000 X-ray diffractometer to study the development of the crystalline phases at different temperatures. Unit cell parameters of $CoFeOPO_4$ and $FePO_4$ structures were measured using LSQC and POWCAL programs [17]. In order to refine "*d*" values, α-Al_2O_3 was employed as an internal standard in an X-ray diffractogram running between 10° and 80° (2θ). When solid solutions were formed, a structure profile refinement was carried out by the Rietveld method [18] with the data obtained between 15° and 80° (2θ). The diffraction patterns were collected using monochromated Cu Kα radiation, a step size of 0.02° 2θ, and a sampling time of 10 s.

In order to test their efficiency as blue ceramic dye, the fired compositions were dispersed (5 wt%) into a transparent glaze (single-firing glaze of composition 0.106 mol K_2O, 0.565 mol CaO, 0.329 mol ZnO, 0.323 mol Al_2O_3, 1.972 mol SiO_2) onto commercial ceramic biscuits. Glazed tiles were fired for 5 min at 1085 °C for the single-firing glaze in a cycle of 60 min (cold-to-cold). The properties of ceramic dyes for porcelain stoneware were also analysed. Thus, the samples were 5 wt% mixed in bulk with porcelain stoneware body (spray-dried powder) and fired for 5 min at 1200 °C in a single-firing cycle of 57 min (cold-to-cold).

A Lambda 2000 Perkin-Elmer spectrophotometer with an illuminant D65, an observer 10, a scan rate of 480 nm/min and a reference sample of MgO was used to obtain the UV–vis–NIR (ultraviolet visible near infrared) spectra in the 200–2000 nm range (diffuse reflectance).

Microstructural observations and microanalysis of fired samples were carried out through a scanning electron microscope, LEO 440. The surface of these specimens was previously carbon coated by sputtering.

Model 2900 MicroMag Alternating Gradient Magnetometer was used to obtain the magnetic response of materials at room temperature. This system uses an alternating gradient field to produce a periodic force on a sample placed in a variable dc field. The sample is mounted on an extension rod attached to a piezoelectric element.

X-Rite spectrophotometer (SP60, an illuminant D65, an observer 10°, and a reference sample of MgO) was used to obtain CIE $L^*a^*b^*$ color parameters on glazed tiles: L^* is the lightness axis (black (0) → white (100)), a^* the green (−) → red (+) axis, and b^* is the blue (−) → yellow (+) axis [19].

3. Results and discussion

Table 1 shows the variation of crystalline phases with temperature in $Co_{1-x}Cu_xFeOPO_4$ ($0 \leq x \leq 1$) compositions.

Table 1
Crystalline phase evolution with temperature in $Co_{1-x}Cu_xFeOPO_4$ samples

Synthesis method	x	Raw sample	800 °C	900 °C	1000 °C
C	0.0	F(s), NP(s), C(m)	F(w), C(vw), FP(w), CoP(w), CP(vw),OP(vw)	OP_{II}(m), CP(vw), FP(vw)	OP_{II}(s)
C	0.1	F(s), NP(s), C(m), Cu(vw)	F(vw), C(vw), FP(w), CoP(w), CP(vw),OP(m)	OP_{II} (m), FP(vw)	OP_{II}(s)
C	0.2	F(s), NP(s), C(m), Cu(w)	F(w), C(vw), FP(w), CoP(w), CP(vw),OP(m)	OP_{II}(m)	OP_{II}(s)
C	0.5	F(s), NP(s), C(m), Cu(m)	F(vw), FP(vw), CoP(w),CuP(w), OP(m), Cu(w)	OP_{II} (m), CuP(w)	OP_{II}(s)
C	0.8	F(s), NP(s), C(w), Cu(m)	F(vw), FP(w), CoP(w),CuP(w), OP(vw), Cu(w)	OP_{II}(m), CuP(m)	OP_{II}(s)
C	1.0	F(s), NP(s), Cu(vw)	F(vw), CuP(w), OP(vw),Cu(vw)	OP_{II} (s) CuP(w)	OP_{II}(s), CuP(w)
G	0.0	NN(s)	OP(vw),CP(vw)	OP(m), CP(w)	OP(s), F(vw), CP(vw)
G	0.1	NN(s)	OP(w), CP(vw)	OP(m), CP(w)	OP(s), F(vw), CP(vw)
G	0.2	NN(s)	OP(w), CP(vw)	OP_{II}(m)	OP(s), F(vw), CP(vw)
G	0.5	NN(s)	OP(w), CP(vw)	OP_{II}(m)	OP(m), CuP(vw)
G	0.8	NN(s)	OP(w), CP(w)	OP_{II}(m)	OP(m), CuP (w)
G	1.0	NN(s)	OP(w), F(w)	OP(m), F(m)	OP(m), F(m)

Synthesis method: C = ceramic method and G = sol–gel method. Crystalline phases: F = Fe_2O_3 (hematite), C = Co_3O_4, Cu = CuO, NP = $(NH_4)_2HPO_4$, NN = NH_4NO_3, OP = $MFeO(PO_4)$ solid solution (M: Co, Fe, Cu), OP_{II} = two crystalline phases with Fe_2OPO_4 structure and with peak position very near, FP = $FePO_4$, CoP = $Co_2P_2O_7$, CP = $Co_3(PO_4)_2$, CuP = $Cu(PO_3)_2$. Diffraction peak intensity: s = strong, m = medium, w = weak, vw = very weak.

From samples prepared by the ceramic method two crystalline phases, with very near position peaks of Fe_2OPO_4 structure are detected at 1000 °C/48 h. These two crystalline phases have been assigned to $MFeOPO_4$ (M = Co, Cu) solid solutions with similar compositions as described in rutile system also [20,21]. In $CuFeOPO_4$ composition ($x = 1$), $Cu(PO_3)_2$ as residual phase is also detected. From samples prepared by the sol–gel method $MFeOPO_4$ (M = Co, Cu) solid solutions are obtained (one crystalline phase) at 1000 °C. $Co_3(PO_4)_2$, $Cu(PO_3)_2$ or Fe_2O_3 are also detected as residual phases at this temperature. Fig. 1 shows X-ray powder diffraction pattern for $Co_{0.2}Cu_{0.8}FeOPO_4$ composition prepared by the ceramic method (two $MFeOPO_4$ phases) and Fig. 2 the Rietveld refinement plot of the X-ray powder diffraction data for $Co_{0.9}Cu_{0.1}FeOPO_4$ composition prepared by the sol–gel method (one $MFeOPO_4$ phase) as representative samples.

Fig. 3 shows the unit cell parameters of Fe_2OPO_4 structure from Rietveld refinements obtained for samples with $Co_{1-x}Cu_xFeOPO_4$ ($0 \leq x \leq 1$) compositions synthesized by sol–gel method and fired at 1000 °C. The variation of these parameters with composition confirms the formation of the $MFeOPO_4$ solid solutions. The increase of the a parameter with x is in accordance with the replacement of Co^{2+} ion by a greater one (Cu^{2+}). The decrease of the b and c parameters with x can be related with changes in distances M–M and M–O (M = Co, Fe, Cu) [22]. These values are intermediate values between unit cell parameters in $CoFeOPO_4$ ($a = 7.2548$ Å, $b = 6.4471$ Å, $c = 7.4570$ Å) and unit cell parameters in $CuFeOPO_4$ ($a = 7.5152$ Å, $b = 6.3948$ Å, $c = 7.1716$ Å) [16].

Fig. 4 shows the UV–vis absorption spectra of the powdered sample with $Co_{0.9}Cu_{0.1}FeOPO_4$ composition and glazed tiles as representative sample. These spectra are also compared with UV–vis spectra of Fe_2OPO_4 compound, $CoFeOPO_4$ compound and $Co_{0.2}Cu_{0.8}FeOPO_4$ composition. From the UV–vis spectra in $Co_{1-x}Cu_xFeOPO_4$ samples with $0 \leq x \leq 1.0$ fired at 1000 °C, three absorption bands are observed about 1200 nm ($^4T_{1g} \rightarrow {}^4T_{2g}$ transition), 638 nm ($^4T_{1g} \rightarrow {}^4A_{2g}$ transition) and 575 nm ($^4T_{1g} \rightarrow {}^4T_{1g}(P)$ transition). These

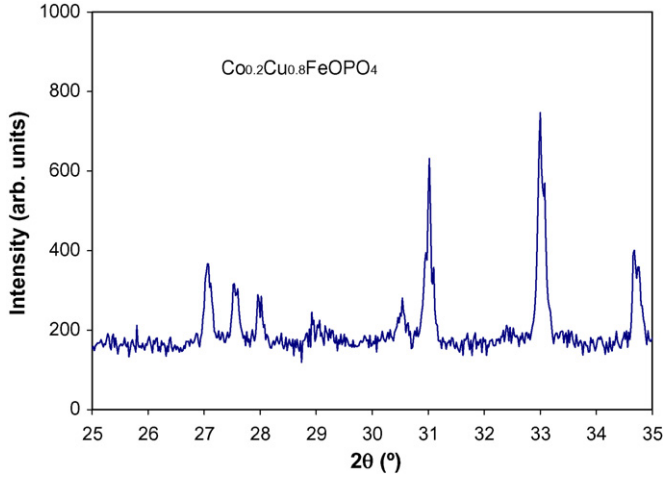

Fig. 1. X-ray powder diffraction pattern for $Co_{0.2}Cu_{0.8}FeOPO_4$ composition prepared by the ceramic method and fired at 1000 °C (biphasic Fe_2OPO_4 structure).

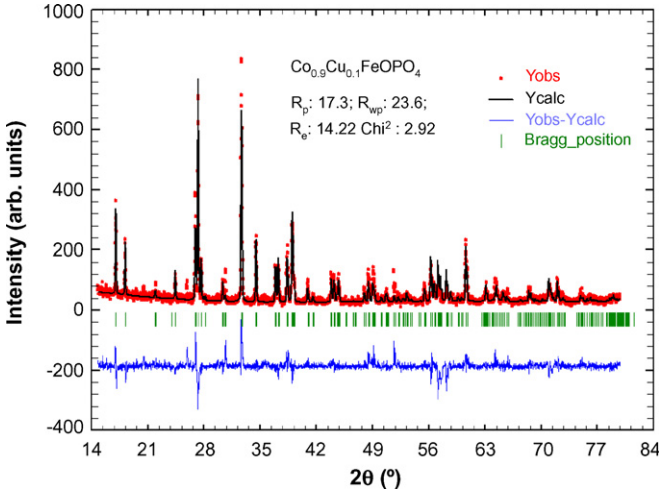

Fig. 2. Rietveld refinement plot of the X-ray powder diffraction data for $Co_{0.9}Cu_{0.1}FeOPO_4$ composition prepared by the sol–gel method and fired at 1000 °C.

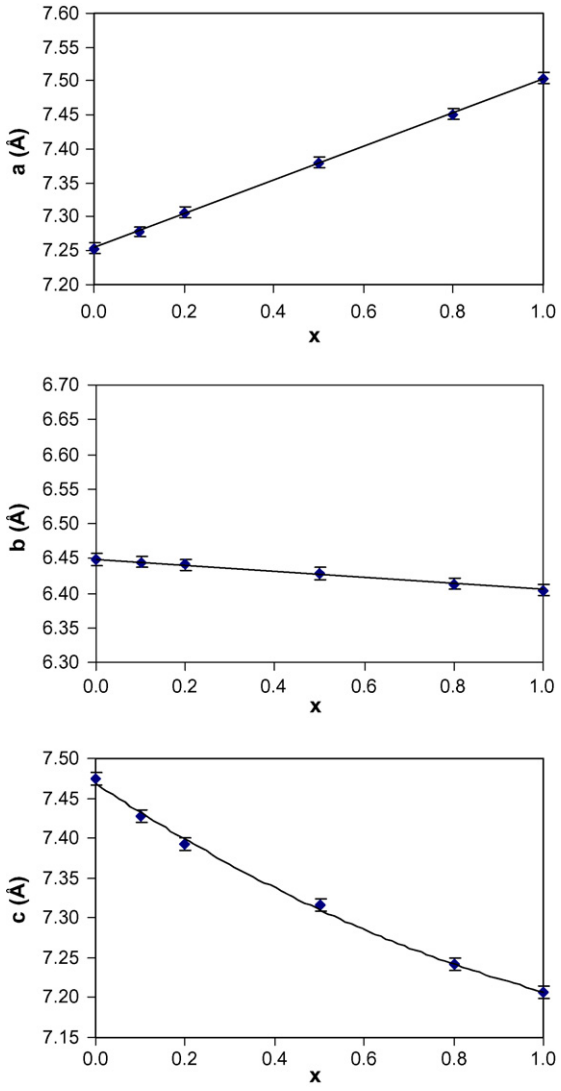

Fig. 3. Unit cell parameters of Fe_2OPO_4 structure obtained from $Co_{1-x}Cu_x$-$FeOPO_4$ compositions synthesized by sol–gel method and fired at 1000 °C.

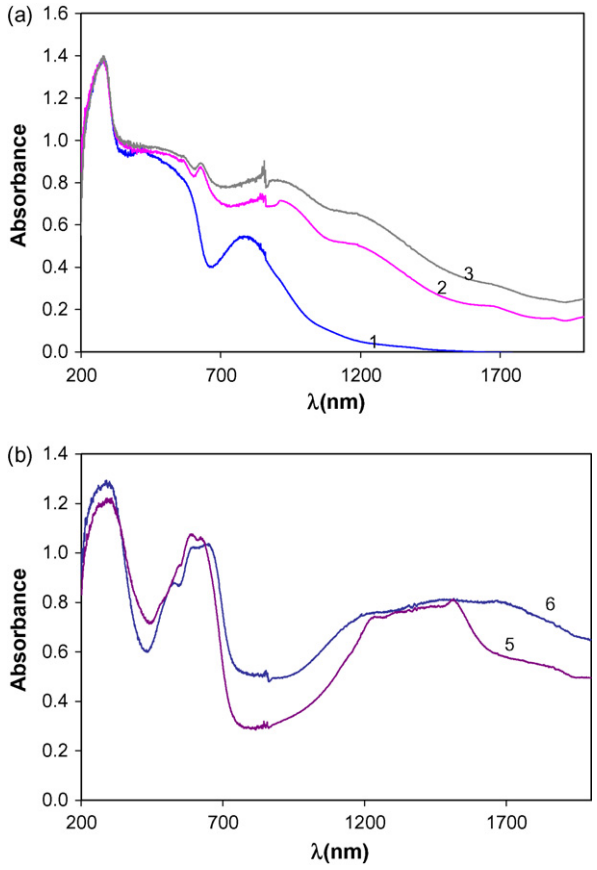

Fig. 4. UV–vis–NIR spectra of $Co_{1-x}Cu_xFeOPO_4$ compositions synthesized by sol–gel method and fired at 1000 °C. (a) Powdered samples: (1) Fe_2OPO_4, (2) $CoFeOPO_4$, (3) $Co_{0.9}Cu_{0.1}FeOPO_4$, (4) $Co_{0.2}Cu_{0.8}FeOPO_4$. (b) $Co_{0.9}Cu_{0.1}$-$FeOPO_4$ sample: (5) with porcelain stoneware, (6) glazed tiles with transparent glaze (single fire) for stoneware.

bands are assigned to Co^{2+} in octahedral site [15] and they fit the Tanabe-Sugano diagram for a *B* value around 720 nm, that implies a quite high degree of covalency of the Co–O bond. The absorbance from Fe^{3+} masks the last one at 575 nm. It is in accordance with the presence of $CoFeOPO_4$ structure detected by XRD. From Fe_2OPO_4 the absorption band at 800 nm is assigned to Fe^{3+} in octahedral site [23]. A strong absorption between 700 and 1600 nm is observed when copper amount is high ($Co_{0.2}Cu_{0.8}FeOPO_4$).

In UV–vis spectra of glazed samples absorption bands of Co^{2+} ion (in a tetrahedral site) mask absorbance from iron and copper. From glazed tiles, three absorption bands are associated with Co^{2+} ion. These bands at 1200–1600 nm ($^4A_2 \rightarrow {}^4T_1(F)$ transition) and a double band with maximal absorption at 640 and 600 nm ($^4A_2 \rightarrow {}^4T_1(P)$ transition) are assigned to Co^{2+} in a tetrahedral site [23].

UV–vis curves indicate a change in Co^{2+} coordination from 6 (powdered samples) to 4 (glazed samples) in all prepared $Co_{1-x}Cu_xFeOPO_4$ samples. It is in accordance with diffusing Co^{2+} ions from their coordination sites in the pigment ($MFeOPO_4$ structure) to tetrahedral sites of the glassy matrix.

SEM/EDX analyses on powdered samples show particle aggregate with compositions according to XRD results. From powdered samples or glazed samples different results are obtained. Fig. 5 shows the existence of Fe-rich particles from EDX mapping in glazed samples. These results confirm that the $MFeO(PO_4)$ (M = Co, Cu) solid solutions are dissolved. The Fe_2OPO_4 structure introduced the Co^{2+} ions into glassy matrix. These ions remain in glassy samples and the blue color of enamelled samples is attributed to Co^{2+} ions.

At 294 K, the variation in saturation magnetization (*M*) with composition decreases with *x* for $Co_{1-x}Cu_xFeOPO_4$ samples. It is in accordance with the substitution of Co^{2+} ions (μ = 4.1–5.2 BM) by Cu^{2+} ions (μ = 1.7–2.2 BM) in the formation of $Co_{1-x}Cu_xFeOPO_4$ solid solutions with Fe_2OPO_4 structure detected by XRD. Samples with $x < 0.2$ prepared from gels presents saturation magnetization higher than the same compositions prepared by ceramic method (Fig. 6). This fact is in accordance with the formation of solid solutions with Fe_2OPO_4 structure. These compositions fired at 1000 °C/2 h with $x < 0.5$ and prepared from gels are ferromagnetic materials and their magnetic hardness decreases with *x*.

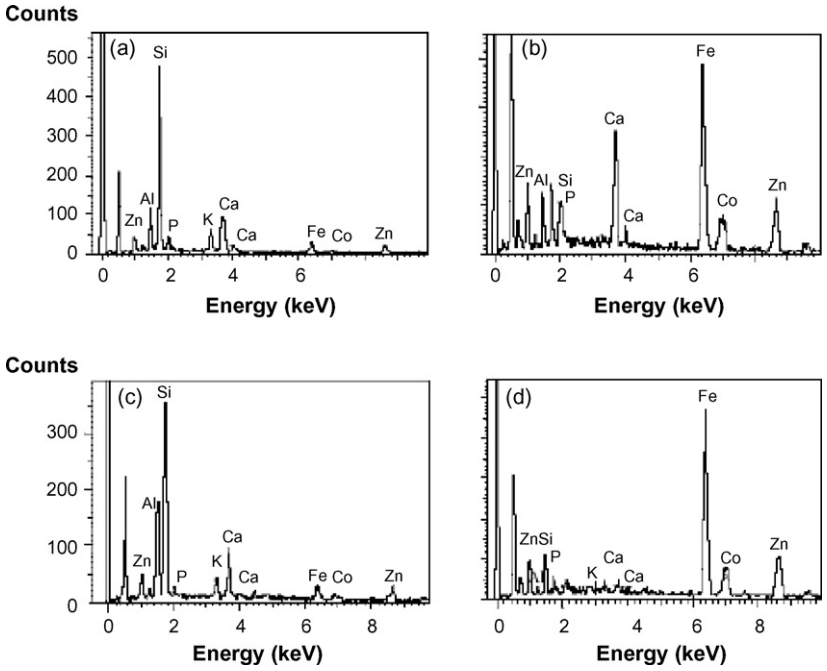

Fig. 5. EDX spectra of tiles from $Co_{0.8}Cu_{0.2}FeOPO_4$ gel sample fired at 1000 °C. Glazed tiles from transparent glaze (single fire) for stoneware: (a) global analyses, (b) spot analyses performed on Fe-rich region. Tiles from porcelain stoneware: (c) global analyses, (d) spot analyses performed on Fe-rich region.

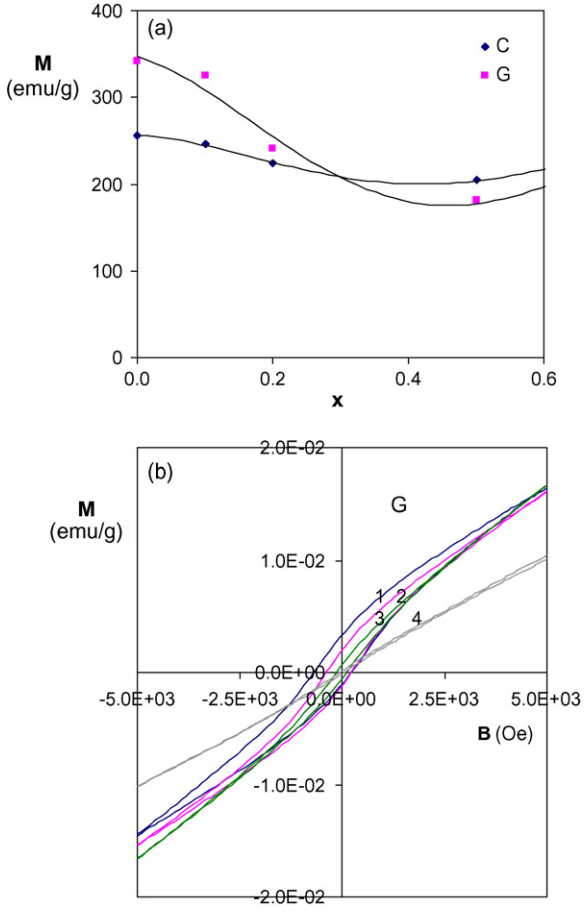

Fig. 6. (a) Variation in saturation magnetization with composition and synthesis method. (b) Magnetic behaviour of $Co_{1-x}Cu_xFeOPO_4$ compositions synthesized by sol–gel method and fired at 1000 °C: (1) $x = 0.0$, (2) $x = 0.1$, (3) $x = 0.2$ and (4) $x = 0.5$.

Composition with $x = 0.5$ shows paramagnetic behaviour. Thus, the incorporation of copper or the decrease of cobalt in solid solutions with Fe_2OPO_4 structure decreases the magnetic hardness of these materials.

Table 2 shows the CIE L^*, a^* and b^* parameters in $Co_{1-x}Cu_xFeOPO_4$ samples fired at 1000 °C and glazed tiles. From these results, it is possible to establish the compositional range for which the suitable blue color is maintained in glazed samples. It is $x \leq 0.5$ in $Co_{1-x}Cu_xFeOPO_4$ compositions (about 13 wt% Co). This nominal Co wt% is comparable with the nominal Co wt% in $Fe_{0.7}Co_{0.3}PO_{3.85}$ compositions (12 wt% Co) obtained in a previous study [15]. The presence of Cu^{2+} in samples changes the CIE L^*, a^* and b^* parameters of glazed tiles. Thus, in $Fe_{0.7}Co_{0.3}PO_{3.85}$ composition 31.99/9.63/−26.3 (transparent glaze) and 47.56/−3.26/−7.94 (porcelain stoneware) were obtained while in the $Co_{0.5}Cu_{0.5}FeOPO_4$ composition 42.23/−3.17/−13.66 (transparent glaze) and 42.73/−4.94/−7.75 (porcelain stoneware) are obtained. Blue materials are desired in this study. In general, the change of color in glazed tiles is not an inconvenient but pinhole defect is obtained from glazed samples when copper amount is high. This defect is associated with decomposition of $MFeOPO_4$. Therefore, $Co_{1-x}Cu_xFeOPO_4$ compositions are not indicated to minimize the Co content in ceramic coloration.

From phase equilibria in the iron oxide-cobalt oxide-phosphorus oxide system reported by De Guire et al. [24], mixtures of $CoFeOPO_4$, $FePO_4$ and $Co_3Fe_4(PO_4)_6$ compounds are obtained from $CoFeOPO_4$–$2FePO_4$ compositions. To investigate the development of suitable blue materials, samples in $CoFeOPO_4$–$2FePO_4$ composition range were prepared ($Co_{1-x}Fe_{1+x}O_{1-x}(PO_4)_{1+x}$). In these samples, Fe/Co/P ratios between 1/1/1 and 2/0/2 are considered to minimize the Co content in materials.

Table 2
CIE $L^*a^*b^*$ ($L^*/a^*/b^*$) color parameters in $Co_{1-x}Cu_xFeOPO_4$ samples

Synthesis method	x	Samples fired at 1000 °C/48 h			Glazed tiles from transparent glaze[a]			Porcelain stoneware		
		L^*	a^*	b^*	L^*	a^*	b^*	L^*	a^*	b^*
C	0.0	41.53	1.56	1.97	42.42	1.66	−19.65	39.54	−0.61	−17.76
C	0.1	42.87	−0.03	1.08	42.24	0.96	−19.87	39.15	−1.83	−13.80
C	0.2	43.76	0.33	1.69	40.41	−0.05	−17.45	39.43	−2.83	−12.61
C	0.5	44.15	0.79	2.73	44.23	−3.65	−13.77	43.30	−5.01	−6.83
C	0.8	44.37	0.46	2.65	47.41	−6.37	−5.51	49.16	−5.59	3.38
C	1.0	44.55	−0.27	2.53	50.11	−7.43	0.41	56.83	−1.86	16.81
G	0.0	41.61	0.47	0.80	43.40	2.49	−22.46	37.85	−0.67	−16.42
G	0.1	42.57	1.71	2.56	41.27	1.08	−19.28	37.51	−1.24	−13.83
G	0.2	43.04	0.60	1.31	40.69	0.17	−17.95	39.52	−2.48	−13.04
G	0.5	43.97	0.97	2.36	42.23	−3.17	−13.66	42.73	−4.94	−7.75
G	0.8	44.21	0.60	2.87	44.50	−5.63	−7.08	49.51	−5.96	2.67
G	1.0	45.19	−0.52	1.53	39.96	−3.26	−4.91	57.98	0.45	18.08

Synthesis method: C = ceramic method and G = sol–gel method.
[a] Transparent glaze (single fire) for stoneware.

Table 3 shows the variation of crystalline phases with temperature in $Co_{1-x}Fe_{1+x}O_{1-x}(PO_4)_{1+x}$ ($0 \le x \le 1$) compositions. From these compositions, mixtures of $CoFeOPO_4$ and $Co_3Fe_4(PO_4)_6$ when $0 < x < 0.5$ and mixtures of $FePO_4$ and $Co_3Fe_4(PO_4)_6$ when $0.7 < x < 0.9$ ($x = 0$: $CoFeOPO_4$; $x = 1$: $2FePO_4$) are obtained. No significative changes in unit cell parameters of $CoFeOPO_4$ structure are detected. Fig. 7 shows the variation of unit cell parameters of $Co_{1-x}Fe_{1+x}O_{1-x}(PO_4)_{1+x}$ obtained by LSQC + POWCAL programs. Results indicate that solid solutions are not formed from these compositions. It is in accordance with De Guire et al. [24].

Colorations of samples fired at 1000 °C are brown when $x < 0.5$ and green when $0.5 < x < 0.9$ depending on the amount of $CoFeOPO_4$ (brown) and $Co_3Fe_4(PO_4)_6$ (green) compounds in samples. The coloration of these powdered samples is not maintained in glazed tiles. It indicates that $CoFeOPO_4$ and $Co_3Fe_4(PO_4)_6$ compounds decompose into glaze. Fig. 8 shows the UV–vis spectra of $Co_{0.5}Fe_{1.5}O_{0.5}(PO_4)_{1.5}$ composition as representative sample. Absorption bands of cobalt and iron in samples are not defined in spectra. A strong absorption between 300 and 1200 nm together to an absorption band about 1700 nm are detected from these compositions. The change of initial coloration to blue

Table 3
Crystalline phase evolution with temperature in $Fe_{1+x}Co_{1-x}O_{1-x}(PO_4)_{1+x}$ samples

x	Raw sample	800 °C	1000 °C
0.0	NN(m)	OP(m), FP(w), CFP (vw)	OP(s)
0.1	NN(m)	OP(m), FP(w), CFP (vw)	OP(s), CFP (vw)
0.2	NN(m)	OP(m), FP(w), CFP (w)	OP(s), CFP (w)
0.3	NN(m)	OP(m), FP(m), CFP (m)	OP(s), CFP (m)
0.5	NN(m)	OP(m), FP(w), CFP (vw)	OP(s), CFP (m)
0.7	NN(m)	FP(s), OP(w), CFP (w)	FP(s), CFP(m)
0.9	NN(m)	FP(s), OP(vw)	FP(s), CFP(m)
1.0	NN(m)	FP(s)	FP(s)

Crystalline phases: NN = NH_4NO_3, OP = $CoFeO(PO_4)$, FP = $FePO_4$, CFP = $Co_3Fe_4(PO_4)_6$. Diffraction peak intensity: s = strong, m = medium, w = weak, vw = very weak.

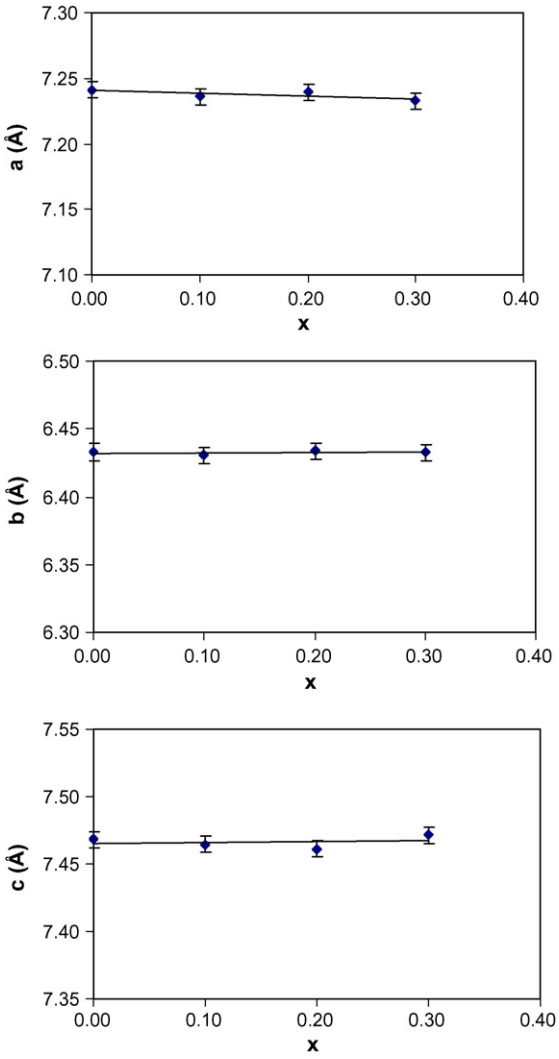

Fig. 7. Unit cell parameters of $Co_{1-x}Fe_{1+x}O_{1-x}(PO_4)_{1+x}$ ($0 \le x \le 1$) synthesized by sol–gel method and fired at 1000 °C.

Table 4
CIE $L^*a^*b^*$ ($L^*/a^*/b^*$) color parameters in $Fe_{1+x}Co_{1-x}O_{1-x}(PO_4)_{1+x}$ samples

x	Samples fired at 1000 °C/48h			Glazed tiles from transparent glaze[a]			Glazed tiles from porcelain stoneware		
	L^*	a^*	b^*	L^*	a^*	b^*	L^*	a^*	b^*
0.0	41.62	1.62	1.79	34.60	2.92	−17.24	36.34	−0.65	−15.10
0.1	42.76	2.49	3.26	33.93	2.03	−14.02	37.70	−1.70	−14.51
0.2	43.34	2.41	4.10	32.41	1.54	−11.18	38.74	−2.22	−13.51
0.3	43.49	1.08	2.99	33.32	1.25	−10.92	41.32	−3.07	−12.36
0.5	44.20	−0.57	2.66	33.74	0.50	−9.05	44.67	−4.14	−9.86
0.7	45.86	−1.95	4.37	42.88	−1.47	−8.80	49.99	−5.33	−5.36
0.9	51.74	−2.34	7.78	48.63	1.01	−0.30	60.18	−4.67	6.43

[a] Transparent glaze (single fire) for stoneware.

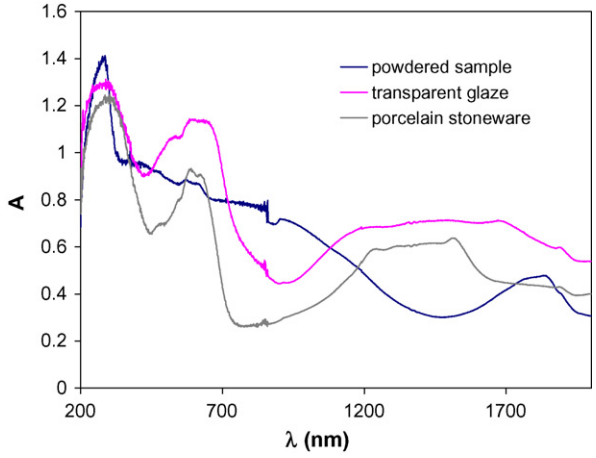

Fig. 8. UV–vis–NIR spectra of $Co_{0.5}Fe_{1.5}O_{0.5}(PO_4)_{1.5}$ sample fired at 1000 °C and applied in glaze and porcelain stoneware body.

coloration in glazed tiles can be seen from the CIE L^*, a^* and b^* parameters (Table 4). A small amount of pinhole defect is obtained from glazed samples when $x < 0.3$. This undesirable effect may be associated with decomposition of $CoFeOPO_4$ and it is only present when the $CoFeOPO_4$ crystalline phase amount is high. Pinholes are not present in samples with $x > 0.3$. Blue materials are obtained when $x < 0.9$. Thus, $0.5 \leq x \leq 0.7$ can be established as optimal composition range to obtain blue glazed tiles from these materials. The nominal Co wt% is 11.2–6.3 in these samples. It is comparable to 12 wt% Co obtained from $Co_{0.3}Fe_{0.7}PO_{3.85}$ composition [15]. In compositions $0.5 \leq x \leq 0.7$ $Co_3Fe_4(PO_4)_6$ crystalline phase amount is high and this structure introduce the Co^{2+} ions into glassy matrix.

Results indicate that an important minimization of cobalt in blue ceramic dyes can be obtained by the incorporation of Co^{2+} ion from phosphates. Optimal cobalt amount is about 10 wt% Co from $Co_{1-x}Fe_{1+x}O_{1-x}(PO_4)_{1+x}$ ($x \approx 0.6$) compositions in the conditions of this study.

4. Conclusions

$MFeO(PO_4)$ (M = Co, Cu) solid solutions have been obtained with $Co_{1-x}Cu_xFeOPO_4$ ($0 \leq x \leq 1$) compositions prepared from gels and fired at 1000 °C/2 h. These compositions with $x < 0.5$ are ferromagnetic materials and their magnetic hardness decreases with x, at 294 K. UV–vis curves indicate a change in Co^{2+} coordination from 6 (powdered samples) to 4 (glazed samples) in all prepared $Co_{1-x}Cu_xFeOPO_4$ samples, according with diffusing Co^{2+} ions from their coordination sites in the pigment ($MFeOPO_4$ structure) to tetrahedral sites of the glassy matrix. The Fe_2OPO_4 structure introduces the Co^{2+} ions into glassy matrix ($MFeO(PO_4)$ (M = Co, Cu) solid solutions). These solid solutions decompose in enamelled samples and pinhole defect is obtained when copper amount is high. Therefore, $Co_{1-x}Cu_xFeOPO_4$ compositions are not indicated to minimize the Co content in ceramic pigments.

From $Co_{1-x}Fe_{1+x}O_{1-x}(PO_4)_{1+x}$ ($0 \leq x \leq 1$) compositions, mixtures of $CoFeOPO_4{\cdot}FePO_4$ and $Co_3Fe_4(PO_4)_6$ are obtained when $0 < x < 1$ ($x = 0$: $CoFeOPO_4$; $x = 1$: $2FePO_4$). $Co_3Fe_4(PO_4)_6$ structure introduce the Co^{2+} ions into glassy matrix. When $0.5 \leq x \leq 0.7$ can be established as an optimal composition range to obtain blue glazed tiles from these materials. In the conditions of this study, optimal cobalt amount is about 10 wt% Co from $Co_{1-x}Fe_{1+x}O_{1-x}(PO_4)_{1+x}$ ($x \approx 0.6$) compositions.

Acknowledgement

We gratefully acknowledge the financial support given by MCYT, MAT 2005-00507 project and by Fundación Caja Castellón, P1-1B2005-06 project.

References

[1] N.V. Russell, F. Wigley, J. Williamson, Microstructural changes to metal bond coatings on gas turbine alloys with time at high temperature, J. Mater. Sci. 35 (2000) 2131–2138.
[2] F. Micciché, E. Oostveen, J. van Haveren, R. van der Linde, The combination of reducing agents/iron as environmentally friendlier alternatives for co-based driers in the drying of alkyd paints, Prog. Org. Coat. 53 (2005) 99–105.
[3] D. Uner, M.K. Demirkol, B. Dernaika, A novel catalyst for diesel soot oxidation, Appl. Catal. B: Environ. 61 (2005) 334–345.
[4] J.A. Weirick, Electrostatic porcelain enameling comes of age, Am. Ceram. Soc. Bull. 57 (6) (1978) 611–612.
[5] M. Frías, M.I. Sánchez de Rojas, Total and soluble chromium, nickel and cobalt content in the main materials used in the manufacturing of Spanish commercial cements, Cement Concrete Res. 32 (2002) 435–440.
[6] W. Cho, M. Kakihana, Crystallization of ceramic pigment $CoAl_2O_4$ nanocrystals from Co-Al metal organic precursor, J. Alloy Compd. 287 (1999) 87–90.

[7] A. Wollenberg, R. Peter, B. Pryzybilla, Multiple superficial basal-cell carcinomas (Basalomatosis) following cobalt irradiation, Brit. J. Dermatol. 133 (4) (1995) 644–646.
[8] K. Lock, S. Becaus, P. Criel, H. Van Eeckhout, C.R. Janssen, Ecotoxicity of cobalt to the springtail Folsomia candida, Comp. Biochem. Phys., Part c 139 (2004) 195–199.
[9] P. Boffetta, Carcinogenicity of trace elements with reference to evaluations made by the International Agency for Research on Cancer, Scand. J. Work Environ. Health 19 (1) (1993) 67–70.
[10] R.K. Mason, Use of cobalt colors in glazes, Am. Ceram. Soc. Bull. 40 (1) (1961) 5–6.
[11] DCMA classification and chemical description of the mixed metal oxide inorganic coloured pigments, Metal Oxides and Ceramics Colors Subcommitee, 2nd ed., Dry Color Manufacturer's Association, Washington, DC, 1982.
[12] S. Eric, L. Kostic-Gvozdenovic, M. Miladinovic, L. Pavlovic, Synthesis of cobalt-based ceramic pigments from industrial waste material, Ceram. Silikaty 34 (1990) 61–67.
[13] M. Llusar, A. Forés, J.A. Badenes, J. Calbo, M.A. Tena, G. Monrós, Colour analysis of some cobalt-based blue pigments, J. Eur. Ceram. Soc. 21 (2001) 1121–1130.
[14] A. Forés, M. Llusar, J.A. Badenes, J. Calbo, M.A. Tena, G. Monrós, Cobalt minimization in willemite ($Co_xZn_{2-x}SiO_4$) ceramic pigments, Green Chem. 2 (2000) 93–100.
[15] S. Meseguer, M.A. Tena, C. Gargori, J.A. Badenes, M. Llusar, G. Monrós, Structure and colour of cobalt ceramic pigments from phosphates, Ceram. Int. 33 (2007) 843–849.
[16] N. El Khayati, R. Cherkaoui El Moursli, J. Rodríguez-Carvajal, G. André, N. Blanchard, F. Bourée, G. Collin, T. Roisnel, Crystal and magnetic structures of the oxyphosphates $MFePO_5$ (M=Fe, Co, Ni, Cu). Analysis of the magnetic ground state in terms of superexchange interactions, Eur. Phys. J. B 22 (2001) 429–442.
[17] POWCAL-LSQC Programmes, Ptt. of Chemistry, Abberdeen University (UK).
[18] J. Rodriguez-Carvajal, Program Fullprof, Laboratoire Leon Brillouin (CEA-CNRS), 2005.
[19] Commission Internationale del'Eclairage, Recommendations on Uniform Color Spaces, Color Difference Equations, Phychometrics Color Terms, Suppl. no. 2, CIE Publication no. 15 (E1-1.31), Commission Internationale del'Eclairage, 1971 (Bureau Central de la CIE, Paris, 1978).
[20] M.A. Tena, M. Llusar, J.A. Badenes, M. Vicente, G. Monrós, Influence of precursors on formation of TiO_2-$CrTaO_4$ rutile solid solutions, Brit. Ceram. T. 99 (5) (2000) 219–224.
[21] M.A. Tena, S. Meseguer, C. Gargori, A. Forés, J.A. Badenes, G. Monrós, Study of Cr-SnO_2 ceramic pigment and Ti/Sn ratio on formation and coloration of these materials, J. Eur. Ceram. Soc. 27 (2007) 215–221.
[22] P. Schmid-Beurmann, Synthesis and phase characterization of a solid solution series between β-$Fe_2(PO_4)O$ and $Fe_4(PO_4)_3(OH)_3$, J. Solid State Chem. 153 (2000) 237–247.
[23] A.B.P. Lever, Inorganic Electronic Spectroscopy, 2nd ed., Elsevier Science B.V., The Netherlands, 1977, pp. 507–511.
[24] M.R. De Guire, T.R.S. Prasanna, G. Kalonji, R.C. O'Handley, Phase equilibria in the iron oxide-cobalt oxide-phosphorus oxide system, J. Am. Ceram. Soc. 70 (11) (1987) 831–837.